DOI: 10.13009/EUCASS2019-604

Design and optimization of glide-back reusable launch vehicle architectures

M. Balesdent [(a)], L. Brevault [(a)], B. Paluch [(b)], R. Wuilbercq [(a)], N. Subra [(a)], R. Thépot[(c)] and A. Patureau de Mirand [(d)]
[(a)] DTIS, ONERA, Université Paris Saclay, F-91123 Palaiseau - France
[(b)] DMAS, ONERA, F-59014 Lille - France
[(c)] DAAA, ONERA, Université Paris Saclay F-92190 Meudon - France
[(d)] CNES, Launchers Directorate, Paris - France

Abstract

In the context of the design of partially reusable launch vehicles, different alternatives may be investigated to recover the first stage while minimizing the costs of reusability and maximizing the performance and reliability. In this paper, a winged configuration of reusable first stage, called glide-back, is studied. This architecture uses the main propulsion system of the first stage to perform a boost-back burn and return to the landing site by a gliding mode using additional lifting surfaces. A focus is made on the design of a reusability kit that can be added to a classical stage to provide it with reusability capabilities. The trade-off between the design of the reusability kit and its impact on the ascent phase, staging point and global performance of the vehicle is investigated through aerodynamics and trajectory analyses.

1. Introduction

In the context of the design and use of partially reusable launch vehicles, different design alternatives may be investigated to recover the first stage while minimizing the costs of reusability and maximizing the vehicle performance and reliability.[12] The toss-back configuration has proven its operational feasibility. Alternative configurations, such as glide-back or fly-back concepts, are worth while to be studied in order to assess the trade-off between different technologies. In this paper, a glide-back configuration is investigated for the first stage. It combines both space and aeronautical technologies to recover the vehicle first stage. The proposed architecture takes-off vertically and lands horizontally. After the lift-off and the first stage ascent mission, the second stage is jettisoned and the first stage reignites a part of its rocket engines to cancel its horizontal velocity. Then, the vehicle performs an aerodynamical reentry and glides back to the landing site. For that purpose, aerodynamical nose, lifting surfaces, gears and corresponding power avionics are added to the initial stage configuration. The overarching aim of this work is to study a "reusability-kit" in order to provide the first stage with both expendable and reusable capabilities. In the context of reusability, the stage can be used several times in reusable mode, and in expendable mode during its final flight. Before lift-off, the kit is mounted on a central core.[2] At the end of the flight, either the kit and the central core are refurbished for the next flight in reusable mode or the kit is removed and installed on another central core if the current core is used for expendable mission. In that way, the reusability kit may be used numerous times as means to lower the costs of access to space.

This study is part of a joint project between the French Space Agency (Centre National d'Etudes Spatiales - CNES) and the French Aerospace Lab (Office National d'Etudes et de Recherches Aérospatiales - ONERA) on Reusable Launch Vehicle (RLV) that started in 2018 and will last until 2020. The goal of this study is to provide a first design for the RLV taking into account the kit integration constraints, the use of LOx/LCH4 PROMETHEUS rocket engine technologies and the specificities of Kourou spaceport operations for winged launch vehicles. In order to estimate the performances of such vehicles, adapted modeling tools and simulations are required through a multidisciplinary approach. In this work, a focus is made on the multidisciplinary process developed in order to assess the performances of the RLV. The results presented in this paper are preliminary results of the conceptual phase for such a winged RLV.

The paper is organized as follows. In Section 2, the design specifications and constraints are presented. In Section 3, the modeling tools and the multidisciplinary process developed for the performance assessments of such a type of vehicles are described. Then, in Section 4, preliminary results are presented. A focus is made on aerodynamics sensitivities to wing geometry and airfoil. Moreover, trajectory analyses are provided with sensitivities to key parameters during the Return To Landing Site (RTLS) phase. Finally, in Section 5, the perspectives of the project are detailed, especially the on-going works.

DOI: 10.13009/EUCASS2019-604

2. Design specifications and constraints

The present study focuses on Two-Stage-To-Orbit with a reusable first stage. It consists in modifying a conventional first stage into a winged RLV. The Ariane-Next configuration is used as a baseline (Figure 1). The mission specifications that have been chosen to perform the design of the glide-back reusability-kit are described in this Section. The goal is to insert a payload of 6.0 metric tons into a 800km circular SSO orbit (Table 1). The vehicle for the reusable mission is a Vertical Take Off - Horizontal Landing configuration. It first lifts off from Kourou carrying out the ascent mission and then returns near to the launch site. Concerning the launch vehicle architecture, the first stage is propelled with 7 PROMETHEUS engines using LOx/LCH4 propellant. The second stage is also propelled with another PROMETHEUS engine. An expendable baseline and an example of a glide-back configuration are illustrated in Figure 1.

Table 1: Summary of mission specifications

Target orbit	SSO, 800km
Launch site	CSG, Kourou, French Guiana
Landing site	CSG, Kourou, French Guiana
Payload mass	6 metric tons
Vehicle type	Two-Stage-To-Orbit (TSTO) reusable vehicle

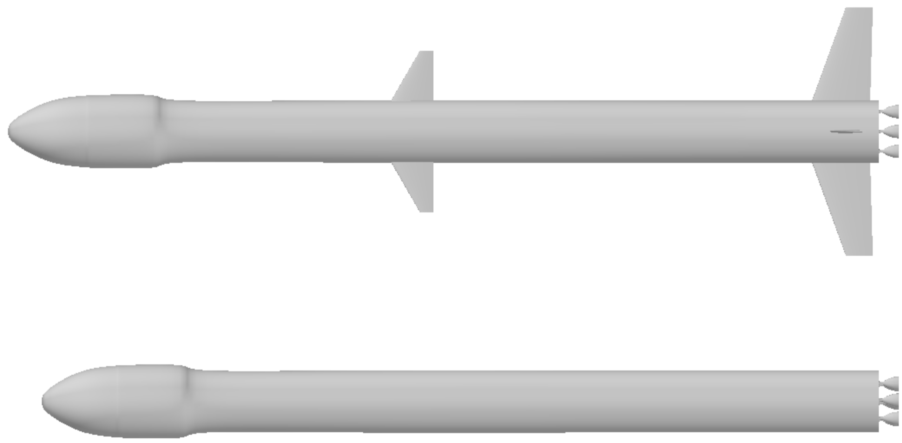

Figure 1: Expendable baseline (bottom) and reusable configuration (top)

The reusability kit is composed of the following components (Figure 2):

- additional lifting surfaces including wings and canards,
- front and rear gears,
- interstage including canards'attachment, front gear integration and required avionics for the first stage,
- vertical stabilizer,
- aerodynamic nose.

The main wings and rear landing gears are located in a reusability pack located in a case that is attached to the main core at the thrust frame (Figure 2). This kit can be removed for the expendable mission. The front landing gear, nose and canards are attached to a skirt located in front of the first stage.

In addition to these specifications, operational constraints on the vehicles are considered. The loads (axial and transverse loads, dynamic pressure and aerothermal flux) during the flights must not exceed a threshold during both the ascent and the return phases. Moreover, safety and visibility constraints near the launch and landing sites are taken into account to ensure the RLV operation safety.

DOI: 10.13009/EUCASS2019-604

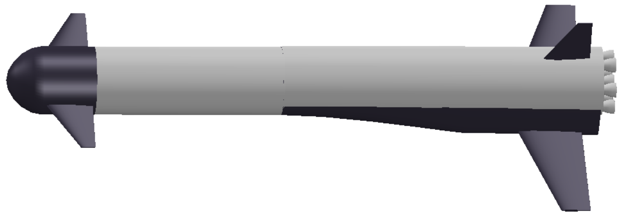

Figure 2: Glide-back configuration with the components of the reusability kit (in black)

3. Models and design process

In this Section, all the disciplines that are used in the design process are briefly described.

3.1 Propulsion

The two stages are propelled by PROMETHEUS engines using LOx/LCH4 propellant.[8] The first stage uses 7 engines and the second stage uses only one engine. The engines are throttable and re-ignitable. The throttling of the engines is exploited for both ascent and return phases in order to respect the maximal axial load constraints. The characteristics and performance of the PROMETHEUS engine are provided by CNES. The thrust varies from 300kN to 1000kN for each engine.[8] The throttling level is optimized during the MDO (Multidisciplinary Design Optimization) process.

3.2 Geometry and sizing

The geometry and sizing discipline allows to model the launch vehicle to provide consistent outputs for the estimation of the aerodynamics (meshes) and the mass budget of the vehicle. This module consists of tools chained together from geometrical modeler to a parametric definition of the vehicle up to the mesh generation for the aerodynamic coefficient estimation. From the main decision variables (length of tanks, planform description of the wing surfaces, *etc.*), the geometry module allows to build a consistent CAD parametric design integrated in the MDO framework. This module gives as outputs meshes for the aerodynamics discipline CFD (Computational Fluid Dynamics) calculations and consistent lengths and scales for mass budget estimation (Figure 3).

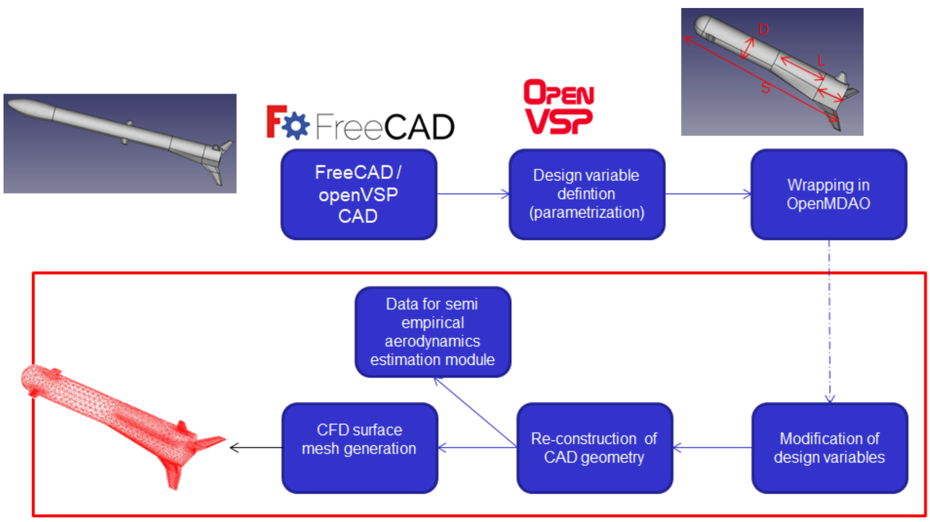

Figure 3: Illustration of geometry discipline

Concerning the mass budget estimation, the masses of the different elements of the stages are predicted using in-house tools developed at ONERA. For the primary structures of the first stage (*e.g.* skirts, tanks, wings), analytical

DOI: 10.13009/EUCASS2019-604

formula and local FEA (Finite Element Analysis) are used to take into account specific aspects such as the distribution of bending moments, buckling, *etc.*. An important matter is to take into account the transversal loads that occurs during the re-entry. These loads are specific to such configurations and have an impact on the design of the overall stage. MER (Mass Estimation Relationships) are mainly used for the secondary structures (*e.g.* gears, equipments, *etc.*). The second stage is designed using standard expendable MER as such a stage is more conventional. This module is integrated as a part of the MDO process to update the mass of the different parts of the stages depending on the loads endured in the flight phases and calculated by the trajectory analysis. The entire chain of geometry and sizing is wrapped into OpenMDAO[6] as a component in order to have the possibility to define some sizing variables as design variables to offer a control by an optimization process.

3.3 Aerodynamics

Estimating with accuracy the aerodynamics behavior of such vehicles is challenging. Indeed, the Mach number and angle of attack vary greatly during the different flight phases occuring during the mission (ascent and re-entry, subsonic, supersonic, hypersonic, propelled phases or not). This requires to use dedicated tools for the aerodynamics coefficient estimation. For that purpose, different tools of various fidelity levels (three in total) have been used. The first level of fidelity consists of two internal low fidelity models (one based on semi-empirical formulations named MISSILE[4] and one based on Local Surface Inclination methods named SHAMAN) that have been implemented to obtain quick estimates of the aerodynamic coefficients. To improve the accuracy of the predictions, specifically for the glide-back flight phase, a second level of fidelity with Euler CFD calculations has been used with an aerodynamic estimation chain based on a derivation on the ONERA's code CANOE[3] relying on SU2.[11] Finally, for the highest level of fidelity, several RANS CFD calculations (Figure 4) have been performed on specific aerodynamics configuration in order to validate the model and to adjust the aerodynamic coefficient estimates. To aggregate the different levels of fidelity, a surrogate model of the previously described models is built via co-kriging techniques.[5,10] This technique uses Gaussian Processes to combine different fidelity models based on the correlation between the model responses. The idea is to build the surrogate model on the higher fidelity model (expensive to evaluate) and enrich it using lower fidelity model (cheaper to evaluate) responses. The outputs of this discipline constitute the aerodynamic models of drag and lift coefficients as functions of the Mach number and the angle of attack. These models have been validated and are used in the trajectory analysis and optimization that follows.

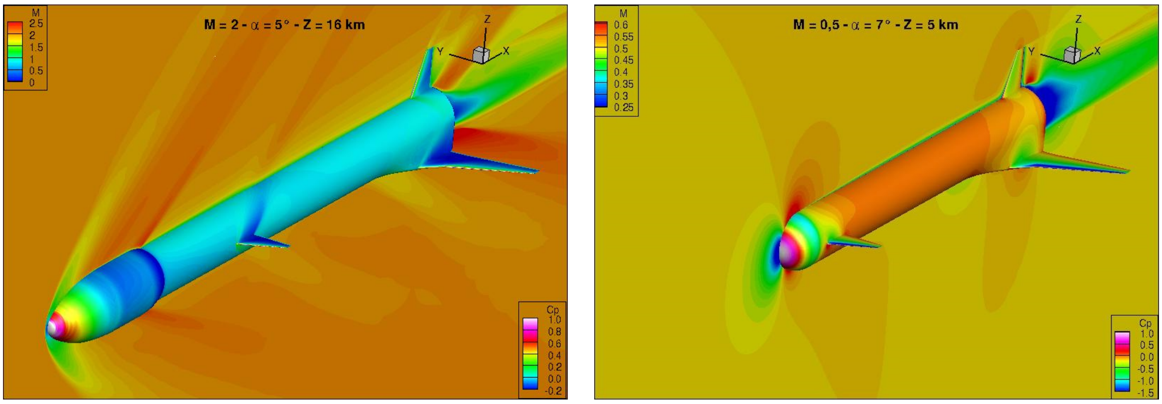

Figure 4: Illustration of CFD RANS calculations: full configuration in supersonic flight (left) and first stage configuration in subsonic glide (right)

3.4 Trajectory

The trajectory discipline aims at finding the optimal guidance law (orientation and thrust level of the engines) to reach the target orbit while satisfying all of the constraints. A three-dimensional rotating Earth frame model is used for the trajectory integration. The ascent trajectory is analog to expendable launch vehicles and is composed of the following phases: first a vertical lift-off, followed by a pitch over maneuver and a gravity turn during the atmospheric flight. Once the exo-atmospheric conditions are reached, the vehicle performs a controlled ascent phase (for both the first and the second stages). Then, a coasting phase (ballistic flight) is considered for the second stage. Finally, a circularization burn is performed at the apogee of the transfer orbit to reach the target orbit, exploiting the re-ignition capability of

DOI: 10.13009/EUCASS2019-604

the PROMETHEUS engine. During the ascent, the pitch angle and yaw angle are optimized using different kinds of control laws depending on the flight phase (pitch over maneuver, controlled phase, *etc.*). The objective is to reach the SSO orbit and minimize the propellant consumption while satisfying the constraints corresponding to the maximal axial and transverse load factors, the maximal dynamic pressure, the maximal angle-of-attack, and the visibility and safety aspects. In order not to exceed the maximal axial load factor, the throttling of the engines is also optimized both for the first and the second stages. The ascent phase and RTLS (Return To Landing Site) strategy for the glide-back mission are illustrated in Figure 5.

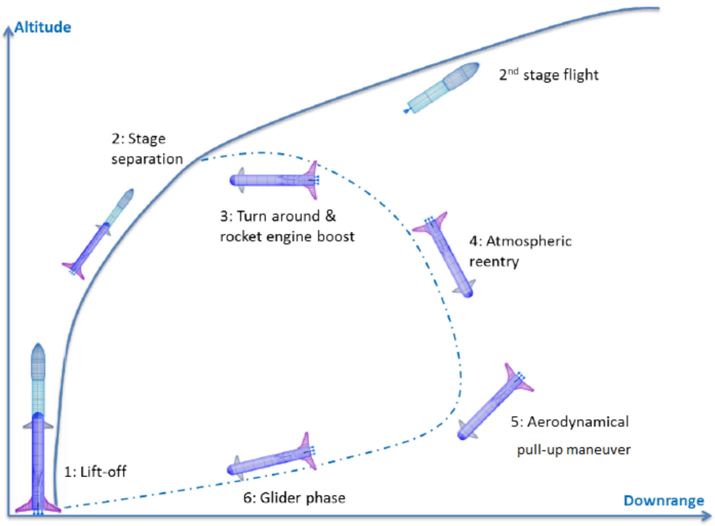

Figure 5: Ascent phase and RTLS by glide-back strategy

With regard to the second phase, once the second stage is jettisoned, the first stage performs a RTLS trajectory composed on the following steps :

- turn around phase: this phase allows to place the stage in an appropriate orientation for the boost-back burn ;
- boost-back maneuver: in this phase, the rocket engines are re-ignited to invert the velocity vector and provide an impulse to the landing site. For this phase, the decision variables are the orientation of the stage (pitch angle and azimuth) as well as the throttling of the engines (only 3 engines are used for this maneuver) ;
- atmospheric re-entry: this phase follows the boost-back maneuver and performs a controlled re-entry to limit the loads ;
- aerodynamical ressource and glide phases: after re-entry, the first stage performs a pull up maneuver and a glide phase to exploit the lifting surfaces to reach the landing site, maximizing the lift-to-drag ratio. The decision variables of this phase are the angle of attack profile and the bank angle profile ;
- final phase: this phase is composed of a turn to align with the runway while satisfying the visibility and safety constraints. The decision variables are analog to the gliding phase.

Figure 6 details the different maneuvers of the RTLS phase. The objective of the optimization process for this phase is to minimize the propellant consumption while satisfying the constraints on the maximal axial and transverse load factors, maximal dynamic pressure and thermal flux during re-entry, maximal angle-of-attack during the glide phase, the maximal velocity at landing, and visibility and safety aspects.

3.5 Design process

All the disciplines have been integrated into an MDO design process using the openMDAO framework developed by NASA and the university of Michigan.[6] To ease the integration process, the WhatsOpt environment developed at ONERA is used.[9] The decision variables are the variables defining the kit (*e.g.*, planforms and profiles of wings and canards), propellant masses of the first stage for both ascent and return phases and propellant masses of the first and

DOI: 10.13009/EUCASS2019-604

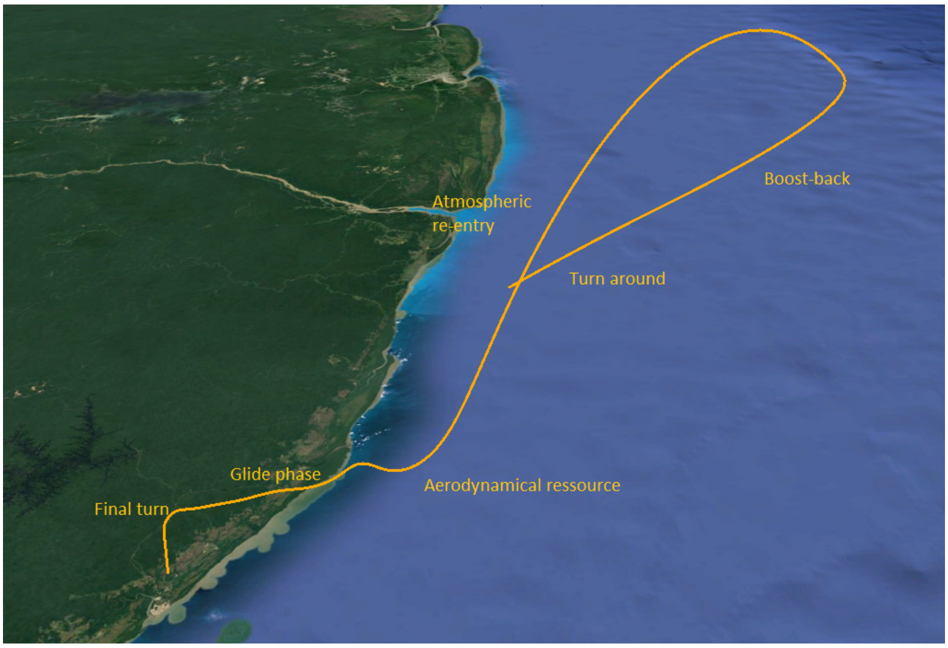

Figure 6: Illustration on the different maneuvers during the RTLS phase

the second stage. A MultiDiscipline Feasible MDO formulation[1] has been implemented (involving Gauss-Seidel Fixed Point Iteration between the different disciplines). The used optimization algorithm is based on the Covariance Matrix Adaptation - Evolution Strategy.[7]

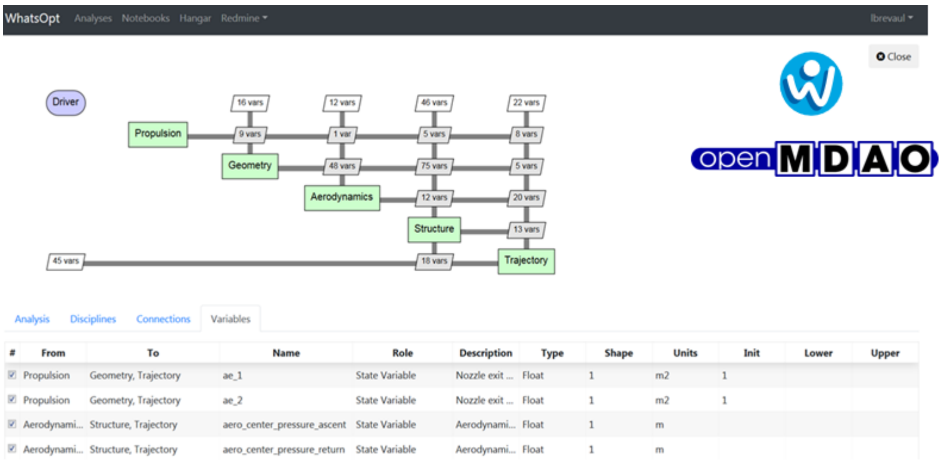

Figure 7: Illustration of the MDO process for the glide-back architecture in the WhatsOpt environment

4. Preliminary analyses

The key drivers for the reusability kit design that are investigated in this paper are the planform and airfoil profile of the wings (Section 4.1), sensitivity to key control parameters of the return trajectory envelop (Section 4.2). More precisely, the return mission is realized by combining a boost-back burn using additional propellant mass and aerodynamics surface for the gliding phase. As the figure of merit for this study is the Gross Lift Off Weight (GLOW), this results in a trade-off between additional propellant mass and structural mass of lifting surfaces of the kit. Moreover, these two components have an important impact not only on the return phase but also on the ascent phase (additional dry mass and drag at ascent).

DOI: 10.13009/EUCASS2019-604

4.1 Sensitivity analyses about wing design

In order to estimate the influence of the wing planform and airfoil, a sensitivity study has been performed for two wing profiles: double wedge and symmetrical NACA (Figure 8). The first tends to present advantages for the supersonic regime whereas the latter is more efficient for the subsonic regime. For this analysis, two aerodynamic databases have been generated (Figure 9) and Lift-over-Drag (L/D) ratio of the configurations have been compared.

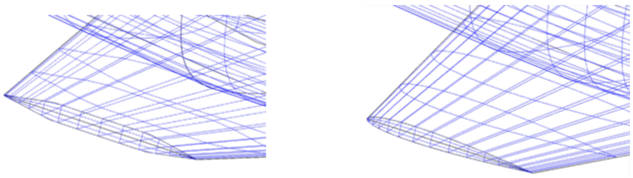

Figure 8: Illustration of double wedge (left) and NACA (right) airfoil profiles for the main wings

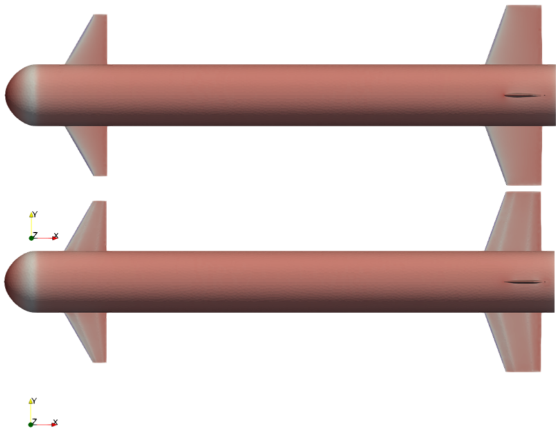

Figure 9: Pressure fields (CFD Euler calculations) for two studied configurations (up: symmetrical NACA, bottom: double-wedge) at subsonic regime (Mach number: 0.5, angle of attack: 5 deg)

Aerodynamic results show a benefit to use NACA airfoil profile due to a better L/D ratio especially in the subsonic regime that is of prime interest concerning the return gliding trajectory (Figure 10). However, the configuration with NACA airfoil profile presents a larger drag in supersonic regime due to the radius of curvature, that can be disadvantageous for the ascent phase inducing more propellant for this phase. Then a global trade-off between the performance for both ascent and return phases has to be performed. The difference in terms of pressure field along the airfoils is illustrated in Figure 9. A coupled analysis between aerodynamics and trajectory optimization is required to assess this trade-off (see next Section). Concerning the wing planform, two different wingspans, corresponding to 3 and 5 times the main core diameter have been studied (the wing share the same root chord, that is set with respect to the thrust frame length). As expected, the L/D ratio for the larger wing presents better characteristics. However, it comes to the cost of increasing the size of the reusability kit and additional space needed on the launch pad for the ground operations and lift-off.

DOI: 10.13009/EUCASS2019-604

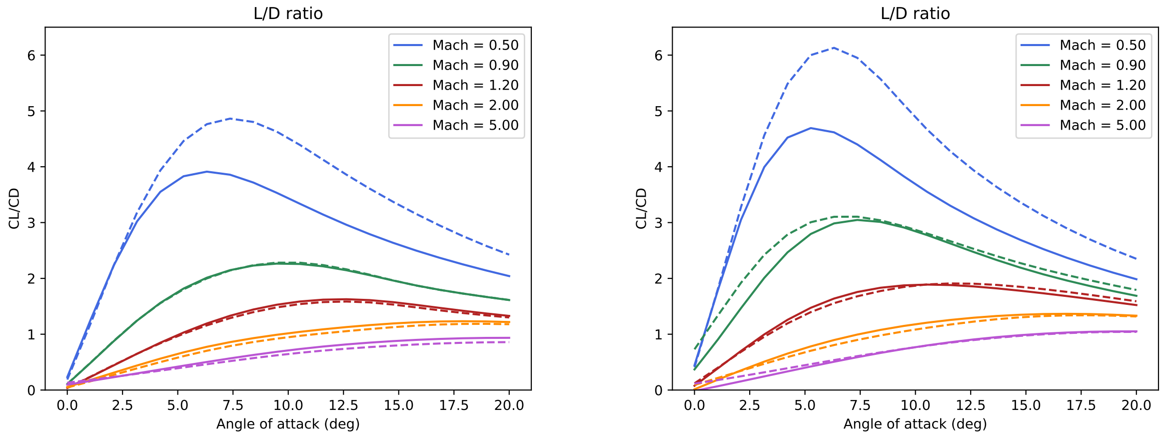

Figure 10: Lift over Drag ratio between NACA (dash line) and double-wedge (solid line) airfoil profiles, as a function of Mach number and angle of attack. Two configurations are evaluated: wingspan equivalent to three times the stage diameter (left), wingspan equivalent to five times the stage diameter (right).

4.2 Ascent and return trajectory profiles

In this Section, results of trajectory optimization are summarized. In these simulations, the NACA airfoil profile is considered (see Section 4.1, with the wingspan equivalent to 5 times the main core diameter). In Figure 11, the altitude profile as a function of time is described, showing the propelled phases for the first and second stages along with the coasting phase allowing to reach the target orbit altitude where a circularization burn is performed.

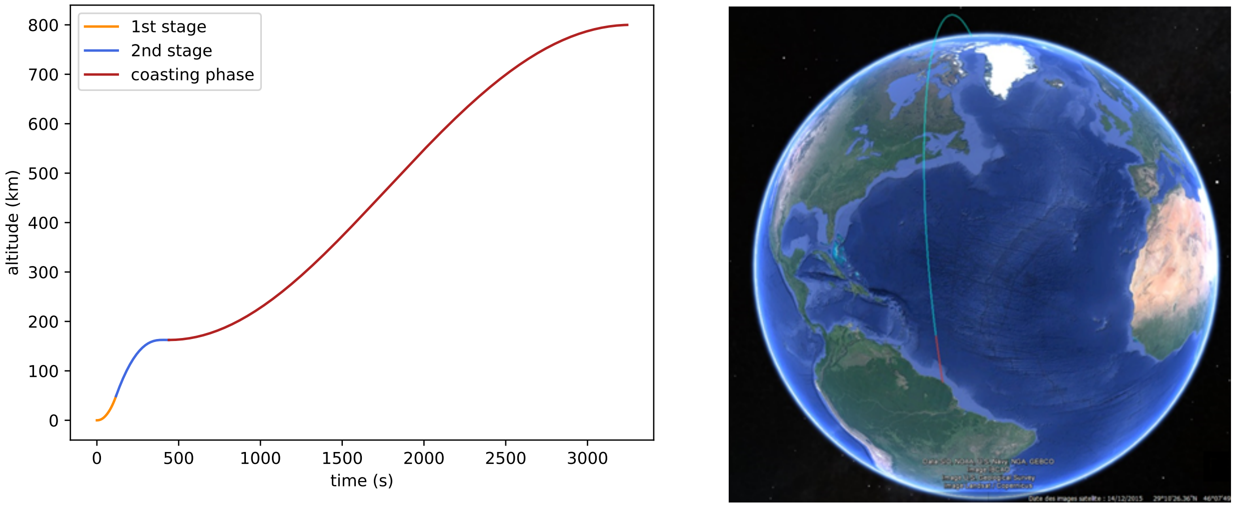

(a) Illustration of the ascent trajectory, altitude as a function of time

(b) Illustration of the ascent trajectory for SSO orbit

Figure 11: Illustration of the ascent trajectory with the propelled and coasting phases

The staging altitude is about 50km and the altitude at the second stage engine cut-off is around 160km. The ascent trajectory for the first stage is mainly driven by the visibility and safety constraints (Figure 12). Due to the load constraints during the ascent, the trajectory of the first stage is performed with a very low angle of attack during the atmospheric phase to keep the transverse loads under the maximal load allowed. The relative low staging velocity is due to the need to bring back the first stage. Indeed, additional propellant mass for the return phase has to be carried out during the ascent phase. This induces a large virtual additional dry mass for the ascent phase that impacts the staging point.

DOI: 10.13009/EUCASS2019-604

The trajectory of the return phase is illustrated in Figure 13. It may be decomposed into three main phases: the turn around phase, the boost-back phase, and the re-entry and gliding phases as depicted in Figure 13a. After staging around 50km of altitude, the turn around phase enables to separate with the second stage and orientate the first stage in order to perform the boost-back burn. Then around 60km of altitude, 3 PROMETHEUS engines are re-ignited, allowing to cancel the horizontal component of the velocity (Figure 13b) and give an impulse toward the landing site. After the engines' cut-off, a ballistic phase with first a parabolic flight with a peak altitude of 100km. Then a re-entry phase is performed at a low angle-of-attack, followed by an aerodynamic pull-up maneuver ending with a gliding phase (starting at a distance of 60km to the landing site and an altitude of around 15km) up to the landing site. At the end of this phase, a final turn is performed using aerodynamic forces to be aligned with the runway (Figure 13c). A sensitivity analysis of the trajectory to the radius of the terminal turn has been performed and is illustrated in Figure 15, while satisfying the safety constraints for the return and landing phases.

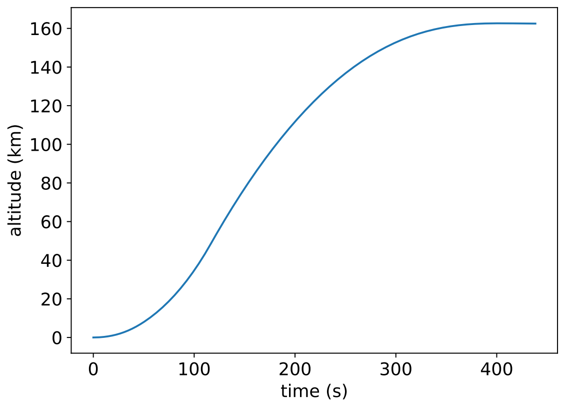

(a) Altitude

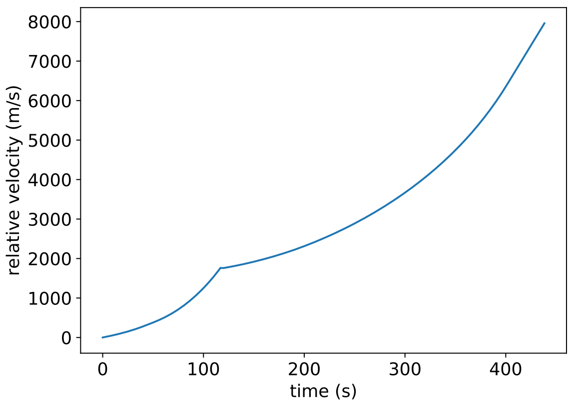

(b) Relative velocity

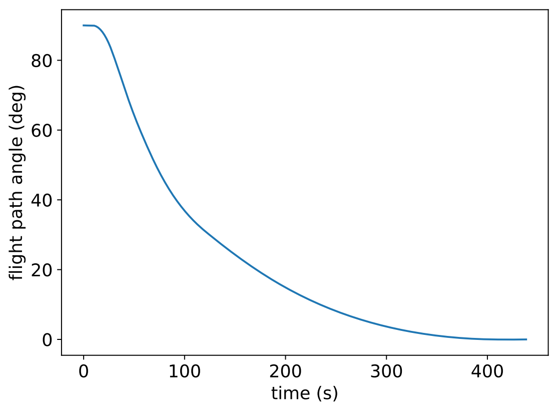

(c) Flight path angle

Figure 12: Illustration of altitude, velocity and flight path angle as a function of time for the ascent propelled phase

With regard to the boost-back phase, two steps may be distinguished, the first one allows to cancel the horizontal component of the velocity (inversion of the velocity vector), the second one enables to orientate the stage toward the landing site. As it can be seen in Figure 13a, the most important part of the boost-back burn is the inversion of the velocity vector. The propellant mass resulting for the impulse to the landing site is very low (Figure 14). This is to be the expected advantage of the glide-back configuration as it uses mainly the lifting surface to perform the return to the landing site mission.

DOI: 10.13009/EUCASS2019-604

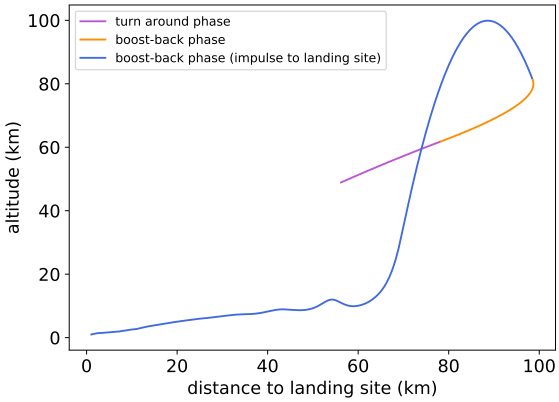

(a) Altitude

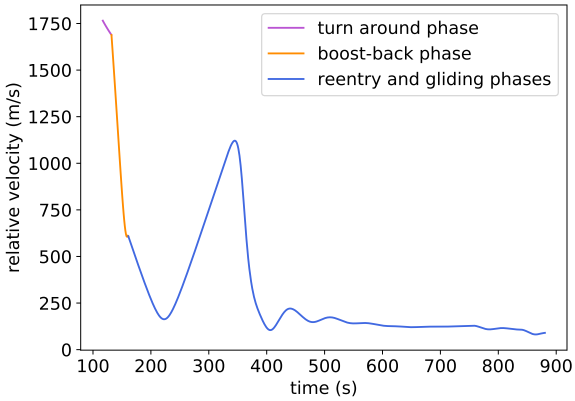

(b) Relative velocity

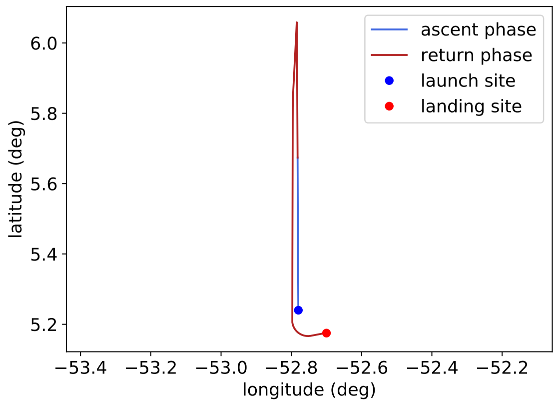

(c) Latitude and longitude

Figure 13: Illustration of generic return trajectory: altitude as a function of distance to the landing site, relative velocity as a function of time, and latitude as a function of longitude

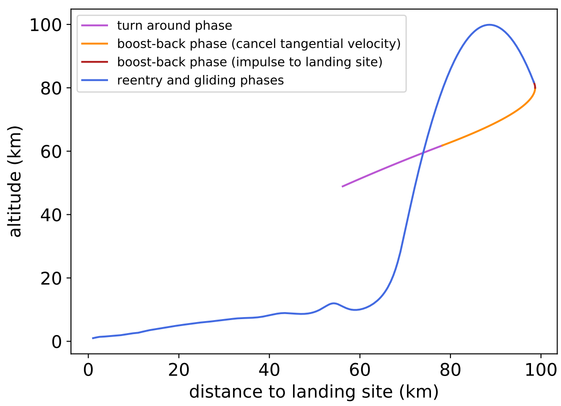

Figure 14: Illustration of the return trajectory, with the different propelled (decomposed into the inversion of horizontal velocity in orange and impulse to the landing site in red) and non propelled phases

DOI: 10.13009/EUCASS2019-604

Finally, a sensitivity analysis about the aerodynamic choices on the entire trajectory has been performed. Figure 16 illustrates the impact of the selection of airfoil profiles (NACA *vs.* double-wedge) on the RTLS phase. As described in Section 4.1 the L/D ratio of the first stage with NACA airfoil profile is larger than with the double wedge profile in the subsonic regime. This impacts the gliding capabilities of the vehicle and therefore the distance where the aerodynamic pull-up maneuver is carried out). This pull-up maneuver is mainly driven by the satisfaction of the maximal transverse load constraints.

Figure 15: Illustration of the sensitivity study to the radius of the terminal turn (yellow: 3km, green: 5km, red: 7.5km, blue: 10km)

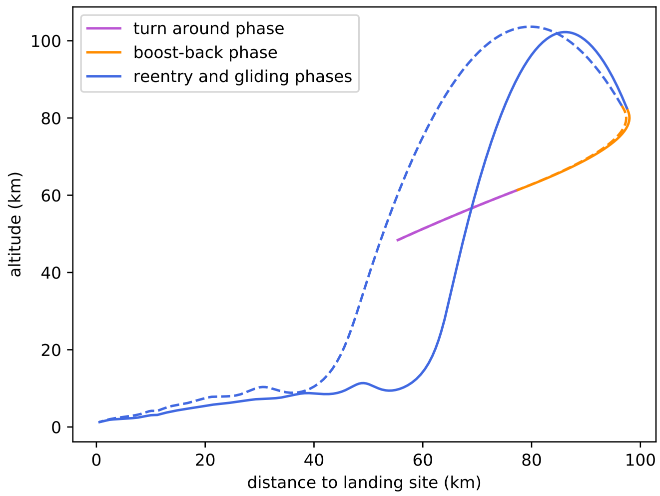

Figure 16: Illustration of return trajectories for the two airfoil profiles described in Section 4.1, altitude as a function of the distance to landing site (in solid line: NACA airfoil profile, in dash line: double-wedge airfoil profile)

5. Conclusion and future works

This paper presents an on-going effort to study the design of a glide-back architecture for the reusability of the first stage. The study is focused on the design of a reusability kit that can be added to the core of a first stage to provide it with reusability capabilities. Preliminary aerodynamic analyses and global trajectory optimizations (ascent and return)

DOI: 10.13009/EUCASS2019-604

involving different configurations of lifting surfaces have been performed in order to assess the trade-off between the size of lifting surfaces, the required additional propellant mass for the return mission and their impact on the ascent phase and global performance of the launch vehicle. Other concepts will be studied in the future, especially a fly-back configuration using additional air-breathing propulsion to perform the RTLS mission.

6. Acknowledgments

The work is funded by the joint project "Programme d'Intérêt Commun - Lanceurs Réutilisables" between CNES and ONERA and by the HERACLES project (Hypersonic Efficient and Reusable Aerospace Concepts for Launcher Evolution Strategies) funded by ONERA.

References

[1] Mathieu Balesdent, Nicolas Bérend, Philippe Dépincé, and Abdelhamid Chriette. A survey of multidisciplinary design optimization methods in launch vehicle design. *Structural and Multidisciplinary optimization*, 45(5):619–642, 2012.

[2] Loïc Brevault, Mathieu Balesdent, Ali Hebbal, and Antoine Patureau De Mirand. Surrogate model-based multi-objective mdo approach for partially reusable launch vehicle design. In *AIAA Scitech 2019 Forum*, page 0704, 2019.

[3] Sebastien Defoort, Michaël Méheut, Bernard Paluch, Romain Liaboeuf, Raphaël Murray, Daniel C Mincu, and Jean-Michel David. Conceptual design of disruptive aircraft configurations based on high-fidelity oad process. In *2018 Aviation Technology, Integration, and Operations Conference*, page 3663, 2018.

[4] Pascal Denis. ONERA's aerodynamic prediction code - MISSILE. In *RTO/AGARD symposium on Missile Aerodynamics, Sorrento*, 1998.

[5] Alexander IJ Forrester, András Sóbester, and Andy J Keane. Multi-fidelity optimization via surrogate modelling. *Proceedings of the royal society a: mathematical, physical and engineering sciences*, 463(2088):3251–3269, 2007.

[6] Justin S. Gray, John T. Hwang, Joaquim R. R. A. Martins, Kenneth T. Moore, and Bret A. Naylor. OpenMDAO: An Open-Source Framework for Multidisciplinary Design, Analysis, and Optimization. *Structural and Multidisciplinary Optimization*, 59:1075–1104, 2019.

[7] Nikolaus Hansen, Sibylle D Müller, and Petros Koumoutsakos. Reducing the time complexity of the derandomized evolution strategy with covariance matrix adaptation (CMA-ES). *Evolutionary computation*, 11(1):1–18, 2003.

[8] Alessandra Iannetti, Nathalie Girard, Nicolas Ravier, Emmanuel Edeline, and David Tchou-Kien. PROMETHEUS, a low cost LOx/CH4 engine prototype. In *53rd AIAA/SAE/ASEE Joint Propulsion Conference*, page 4750, 2017.

[9] Rémi Lafage, Sébastien Defoort, and Thierry Lefebvre. Whatsopt: a web application for multidisciplinary design analysis and optimization. In *AIAA Aviation forum 2019*, 2019.

[10] Loic Le Gratiet and Josselin Garnier. Recursive co-kriging model for design of computer experiments with multiple levels of fidelity. *International Journal for Uncertainty Quantification*, 4(5), 2014.

[11] Francisco Palacios, Thomas D Economon, Aniket Aranake, Sean R Copeland, Amrita K Lonkar, Trent W Lukaczyk, David E Manosalvas, Kedar R Naik, Santiago Padron, Brendan Tracey, et al. Stanford university unstructured (su2): Analysis and design technology for turbulent flows. In *52nd Aerospace Sciences Meeting*, page 0243, 2014.

[12] J Vila and A Patureau de Mirand. Weighting options for the next generation of ariane launchers IAC-17-D2. 4.2. In *68th International Astronautical Congress (IAC), Adelaide, Australia*, pages 25–29, 2017.